UDC 669 . 14 . 018 . 821 : 620 . 193 . 2 : 546 . 726

$Fe(O,OH)_6$ Network Structure of Rust Formed on Weathering Steel Surfaces and Its Relationship with Corrosion Resistance

Masao KIMURA*1 Tamaki SUZUKI*1
Genichi SHIGESATO*1 Hiroshi KIHIRA*1
Koji TANABE*2

Abstract

Weathering steel, when exposed outdoors for a few years, forms a protective layer resulting in reduction of the corrosion rate. The state of rust is fundamental for understanding its mechanism, but the structure and its relationship with the mechanism have not been understood. In this study, a new approach was applied to reveal the nano-structure of rust using x-ray absorption fine structure (XAFS) analysis, X-ray anomalous scattering, reverse Monte-Carlo method, and transmission electron microscopy (TEM). It has been shown that the "$Fe(O,OH)_6$ network" composed of octahedrons of FeO_6 octahedrons evolves during the process of corrosion and that a small amount of additional elements changes its process and affects the final morphology.

1. Introduction

A weathering steel is low-alloy steel to which corrosion resistant elements, mainly Cu and P, are added[1,2]. It is characterized that, after a few years' use without painting, protective rust forms on surfaces to significantly reduce the rate of corrosion. The rust formed on the surfaces of the weathering steel is divided into two layers under observation through a polarization microscope; an inner layer on the steel substrate side is a rust layer not showing polarization (dark layer), and it has been confirmed that Cu and P are enriched there[3,4]. However, no direct and quantitative information regarding the structure of the inner rust layer has been made available, and its historical change has not been studied in detail, either; the lack of information has made clarification of corrosion protection mechanisms difficult. Clarification of corrosion resistance mechanisms of addition elements, however, is very important for quantifying environmental conditions under which the weathering steel is used and estimating long-term service life of the structures of the weathering steel.

For the purpose of clarifying the corrosion protection mechanisms, the authors addressed quantitative analysis of the structure of rust forming on the surfaces of the weathering steel from the standpoint of viewing the structure as a network of $Fe(O,OH)_6$ composed of $Fe(O,OH)_6$ units and as a result, it was made possible to comprehensively understand the structure of weathering steel rust including its secular change. This paper reports the analysis results.

2. Experiments

Chemical compositions of specimens: the weathering steel (WS), mild steel (MS) and binary alloy steel (CR) are shown in **Table 1**, and powder specimens (α-FeOOH and γ-FeOOH) were prepared. Short-term and long-term corrosion tests (from a few weeks to 30 years) were carried out for the purpose of observing historical changes

Table 1 Chemical composition of specimens

Specimen	Composition (mass%)						
	Cu	Cr	Ni	Mn	P	Si	C
WS	0.28	0.55	0.15	0.49	0.081	0.51	0.10
MS	--	-	--	0.60	0.020	0.30	0.15
CR	--	5.00	--	-	-	-	-

WS: weathering steel, MS: mild steel, CR: Fe-5wt%Cr alloy

*1 Technical Development Bureau
*2 Nippon Steel Technoresearch Corporation

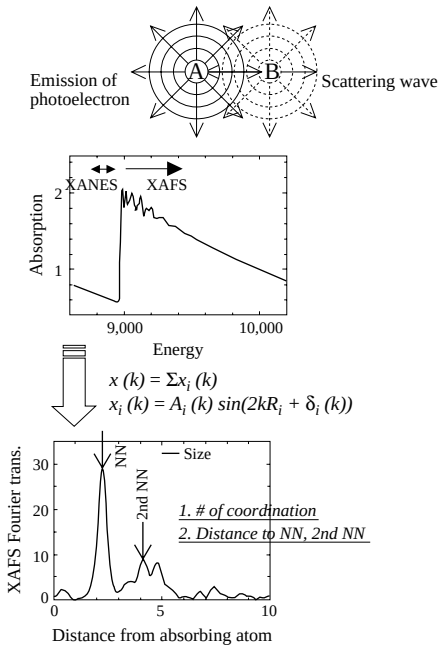

Fig. 1 Principle of XAFS method
(When the energy-dependency of X-ray absorption ratio of an atom of element A is measured, oscillation is observed near an absorption edge owing to interference with a neighboring atom of element B. The distance between the atoms and the number of the atoms are obtained through analysis of the oscillation.)

of rust layers during corrosion progresses. In the short-term corrosion test, the specimens were immersed in artificial seawater for a prescribed period and the rust having formed during the period was collected. In the long-term corrosion test, the specimens were exposed to a rural outdoor environment for a prescribed period.

Sectional thin film test pieces of the specimens were prepared through the focused ion beam (FIB) method for microscopic structure observation, and their structure was observed using a transmission electron microscope (TEM).

In order to obtain quantitative information on the crystal structure of rust (or the network of $Fe(O,OH)_6$), the structure was analyzed employing the analysis techniques named below which are sensitive to the following two levels of atomic correlation:

(a) Short-range order (SRO), which is the correlation in a distance range of approximately 1 nm or less, was investigated using the X-ray absorption fine structure (XAFS) method[5]. The principle of the XAFS method is shown in **Fig. 1**. The investigation was carried out on the beam lines BL-7C, 9A and 12A at the Photon Factory of KEK in Tsukuba, Japan[6,7].

(b) With regard to middle-range order (MRO), which is the correlation in a distance range from 1 to 10 nm or so, precision structural analysis was carried out[8] employing the powder diffraction measurement method using an X-ray diffractometer (line sources: Cu-Kα and Mo-Kα), the anomalous X-ray scattering method[9] using synchrotron radiation, and the reverse-Monte-Carlo (RMC) method[10].

3. Test Results

3.1 Microstructure of rust

Fig. 2 shows a TEM observation image of the interface between rust and the steel substrate at an anodic corrosion portion of a specimen WS exposed to a normal atmosphere for 31 years. Light layers and dark layers were found locally, laminated one on the other (see Fig. 2(a)), and an EDS analysis disclosed that Cr was enriched (Cr concentration of 5 to 10 mass %) in the light layers while it was little contained in the dark layers. Whereas the electron diffraction pattern of the rust portion where Cr is not enriched is in sharp rings, in that of the rust portion where Cr is enriched the diffraction rings are broad (see Fig. 2(b)). It is estimated from the above that the rust in the Cr-enriched portion is in fine particles 2 to 10 μm or so in grain size and its MRO and LRO are in a disordered state.

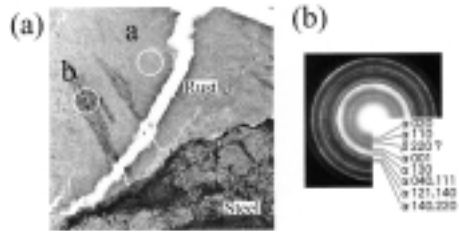

Fig. 2 TEM observation of rust/steel interface of specimen WS after 31 years of corrosion in normal atmosphere
(a) Micro-structure, (b) Diffraction pattern from point "a" in photo (a)

3.2 Results

3.2.1 SRO analysis of rust by XAFS method

Fig. 3 shows the radial distribution functions (RDF) around Fe of the binary alloy specimens (CR) after 2 weeks and 15 years of corrosion measured by the XAFS.

The first peak in the RDF of the colloidal specimen after 2 weeks of corrosion (CR2W(wet)) corresponds to the nearest neighbor of Fe-O [Fe-O(1st NN)], and its second peak corresponds to the nearest neighbor of Fe-Fe [Fe-Fe(1st NN)] and the second nearest neighbor of Fe-O [Fe-O(2nd NN)]. This indicates that $Fe(O,OH)_6$ unit nuclei corresponding to the γ-FeOOH phase were formed at an initial stage of corrosion.

When the colloidal rust is dried (CR2W(dry)), the strength of the third peak ([Fe-Fe(1st NN)] and [Fe-O(2nd NN)]) of its RDF near r = 0.33 nm is increased. This indicates that the $Fe(O,OH)_6$ unit nuclei having formed in the state of a colloid have grown during the drying process.

The RDF of the binary alloy specimen after 15 years of corrosion (CR15Y) is similar to that of the crystalline α-FeOOH specimen. It was made clear from these results that the Fe(O,OH)6 network develops, and a change from γ-FeOOH to α-FeOOH takes place during a long period of corrosion under repeated cycles of wetting and drying (see **Fig. 4**).

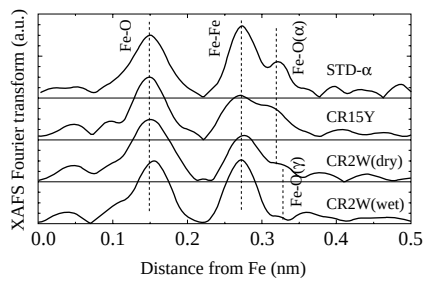

Fig. 3 XAFS radial distribution functions around Fe of binary alloy specimens CR after 2 weeks and 15 years of corrosion (CR2W and CR15Y, respectively) and that of powder α-FeOOH

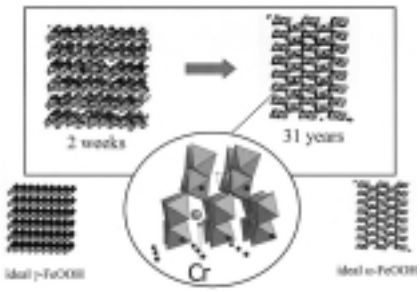

Fig. 4 Change of $Fe(O,OH)_6$ network structure of rust formed on weathering steel
(Only FeO_6 octahedrons are shown for simplicity's sake.)

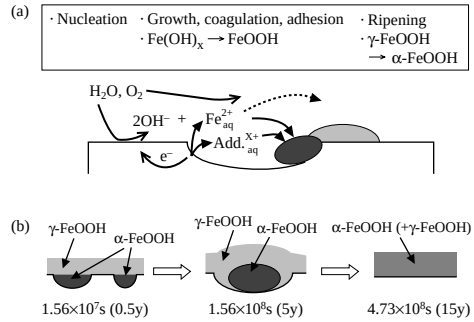

Fig. 5 Rust formation processes in atmospheric exposure environment (a) Common corrosion model, (b) Corrosion model for weathering steel

Conventional weathering steels contain small amounts of Cu, P and Cr. While a Cr addition is believed effective for enhancing corrosion resistance in a low salt environment (a deposition of airborne salt of 0.05 mg-NaCl/dm^2/day or less), there are reports to the effect that it accelerates corrosion in locations where the deposition of airborne salt is large[11]. For developing a reliable weathering steel, while it is necessary to clarify the corrosion protection mechanism of Cr addition, there are many arguments[4,12,13] and the issue has not been made clear.

Facing the situation, the authors carried out a detail analysis by the XAFS method for verifying the involvement of Cr in the formation of the $Fe(O,OH)_6$ network during corrosion processes. As a result, it was revealed that, although Cr formed $Cr(O,OH)_6$ units, like the $Fe(O,OH)_6$ units of Fe, the sites Cr occupied in the network structure of $Cr(O,OH)_6$ were different from the sites Fe usually occupied in the $Fe(O,OH)_6$ network structure (see Fig. 4). Thus, it became clear that the $Cr(O,OH)_6$ compound was not Cr-substituted goethite[12], in which the Fe sites in α-FeOOH were partially substituted with Cr[10,14,15].

3.2.2 Analysis of MRO and network structure of rust by anomalous scattering method

The structures of the rust formed on the CR, WS and MS specimens after 2 weeks and 31 years of exposure were examined by the anomalous scattering measurement and RMC method. Fig. 4 shows the change in the $Fe(O,OH)_6$ network structure of rust formed on the surfaces of the WS specimens. Although the network structure of rust formed after 2-week corrosion is similar to that of the γ-FeOOH phase, the arrangement of $Fe(O,OH)_6$ octahedron units is more in disorder than that in the crystalline phase. In contrast, the network structure of rust formed after 31-year corrosion is similar to that of the α-FeOOH, and the arrangement of the $Fe(O,OH)_6$ octahedron units is more in order. This indicates that the network structure of the $Fe(O,OH)_6$ units changes under repeated cycles of wetting and drying during a long period of exposure to atmosphere, forming a network structure similar to that of the α-FeOOH.

4. Discussion

The environment of the atmospheric exposure consists of repeated cycles of wetting by rain and condensation and drying by the sun and wind, and temperature change constitutes an additional factor. It is conjectured that, in the cycles, dissolved Fe ions turn into $Fe(OH)_x$, separate out from the solution, and finally form rust layers through grain growth (see **Fig. 5**(a)).

As a result of the above examination, the following reactions were found to occur during a long-term exposure of weathering steel. At the very beginning of corrosion, dissolved metal ions form colloidal corrosion products through nucleation and grain growth, and the structure of γ-FeOOH type $Fe(O,OH)_6$ units is formed at this stage. Thereafter, anodic corrosion reactions proceed mainly at the concaves in the steel substrate/rust interface during the cycles of wetting and drying, and the enrichment of addition elements occurs at the anodic corrosion portions. At the same time, the network structure of the $Fe(O,OH)_6$ units changes to form the network structure similar to that of the α-FeOOH (Fig. 5(b)).

The study of the authors further clarified another change in the $Fe(O,OH)_6$ network structure, which constitutes the microstructure of rust. The mechanism by which the corrosion resistance of a weathering steel is realized is examined below from the viewpoint of the change in the network structure (see **Fig. 6**)[10].

The corrosion in the environment of atmospheric exposure can be interpreted as the reactions whereby the metal ions dissolved during the wetting/drying cycles turn into $Fe(OH)_x$, precipitate from the solution, and finally form rust layers through grain growth. Viewing the reactions simply as a combination of two reactions of the separation (precipitation) and grain growth, the rate of the whole reactions can be expresses by the following equation:

$$\nu = N \exp(-E_{Nucl.}/kT) \exp(-E_{Growth}/kT) \quad (1)$$

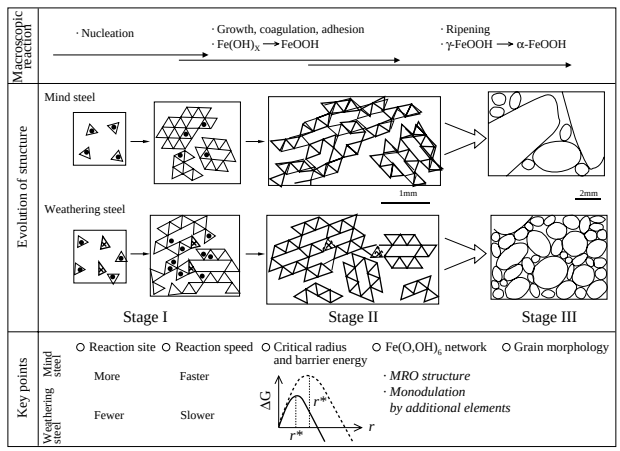

Fig. 6 Mechanisms of corrosion reactions in atmospheric exposure environment
$Fe(O,OH)_6$ network structure seen in initial and middle corrosion stages, crystal structure seen in final corrosion stage (mild steel: upper row, weathering steel: lower row), and predominant factors influencing reactions at different stages.

where N is the number of reaction sites to form the nuclei, and $E_{Nucl.}$ and E_{Growth} are the activation energies of the precipitation and grain growth, respectively. The change in free energy $\Delta G_{Nucl.}$ resulting from the nucleation is a function of the radius r of a formed nucleus and the value of r with which the value of $\Delta G_{Nucl.}$ hits a maximum is the critical radius r^*.

It has been confirmed that the formation of the $Cr(O,OH)_6$ units in the $Fe(O,OH)_6$ network structure of the rust on a weathering steel causes a distortion in the rust structure. In other words, addition of Cr is considered to lead to (a) an increase in the number N of nucleation sites as heterogeneous points and (b) a decrease in the critical radius r^* through a structural distortion of the $Cr(O,OH)_6$ units. As a consequence to the above understanding, it is presumed, nucleation occurs at many sites and the crystal grains finally formed on the weathering steel are fine and have a continuous size distribution (see Fig. 6).

It is understood that the above reactions are quite different in a weathering steel and a mild steel, especially during the development of the $Fe(O,OH)_6$ network structure, and that there is a significant difference in the morphology of the rust finally formed on them, especially in the grain size distribution of the crystals. In other words, the addition elements are considered to modify the $Fe(O,OH)_6$ network structure to change its elementary reactions. As a result, when weathering steel is exposed to the atmosphere, protective rust is formed and high corrosion resistance is created.

It is through the examination of the change in the $Fe(O,OH)_6$ network structure described above that it became possible, for the first time, to clarify the influences of addition elements over corrosion processes. In conventional weathering steels, addition elements (Cu and Cr) so modify the development process of the network structure that a fine and compact structure is finally formed.

It is understood that, under a low salt environment condition (a deposition of airborne salt of 0.05 mg-NaCl/dm^2/day or less), the weathering properties of Cr addition type weathering steels are realized by accelerating the nucleation of colloidal rust and through this, the consequent formation of compact rust. This mechanism is realized thanks to the fact that the chemical activity of Cr is high and it easily forms oxy-hydroxides through hydrolysis. In a high airborne salt environment such as at coastal locations, however, since the hydrolysis reaction expressed by equation (2) below overshoots beyond an effective limit, the pH value is lowered at corrosion surfaces and the progress of corrosion is accelerated. For this reason, addition of Cr is detrimental to the corrosion resistance in a high salt environment.

$$Cr^{3+} + 3H_2O \rightleftarrows Cr(OH)_3 + 3H^+ \quad (2)$$

A new type 3%-Ni weathering steel has been developed, wherein the pH value does not easily fall even in a high salt environment and a rust layer possessing an ion selection function to render chloride harmless is formed[11]. The network structure of the 3%-Ni weathering steel is considered, different from that of conventional weathering steels, to have the ion selection function in addition to a compact structure as a result of Ni addition.

Examination of corrosion reactions from the viewpoint of the $Fe(O,OH)_6$ network structure of rust as delineated above made it possible to clarify corrosion mechanisms, especially the influences of addition elements. The clarification of the mechanisms by which addition elements improve corrosion resistance of steel materials is very important for quantifying environmental conditions under which the weathering steel is used and estimating long-term service life of structures and thus, is indispensable for development of highly reliable materials.

5. Acknowledgements

The authors express sincere gratitude to Prof. Masaharu Nomura and Prof. Tadashi Matsushita of Photon Factory, KEK, for their support in the synchrotron experiments. A part of the studies described herein[8] was carried out under cooperation of Prof. Yoshio Waseda of Tohoku University, for which the authors also express their gratitude.

References

1) Larabee, C. B., Coburn, S. K.: Int. Congress on Metallic Corrosion, London, U.K., 1962, p.276
2) Matsushima, I.: Low-Alloy Corrosion Resistant Steel. Chijin Shokan, 1995
3) Okada, H., Hosoi, Y., Yukawa, K.: J. Iron Steel Inst. Japan (Tetsu-to-Haganè). 55, 355 (1969)
4) Okada, H., Hosoi, Y., Yukawa, K.: J. Iron Steel Inst. Japan (Tetsu-to-Haganè). 56, 277 (1970)
5) Udagawa, Y.: X-ray Absorption Fine Structure. (Gakkai Shuppan Center, 1995
6) Nomura, M., Koyama, A.: X-ray Absorption Fine Structure, Edited by Hasnain, S. S., Ellis Horwood, London, 1991, p.667
7) Nomura, M.: J. Synchrotron Rad. 5, 851 (1998)
8) Kimura, M., Suzuki, T., Sigesato, G., Saito, M., Suzuki, S., Kihira, H., Tanabe, K., Waseda, Y.: J. Japan Inst. Metals. 66, 166 (2002)
9) Waseda, Y.: Novel Application of Anomalous X-ray Scattering for Structural Characterization of Disordered Materials. Springer-Verlag, Heidelberg, 1984
10) McGreevy, R. L., Pusztai, L.: Mol. Simulation. 1, 359 (1988)
11) Kihira, H., Ito, S., Mizoguchi, T., Murata, T., Usami, A., Tanabe, K.: Zairyo-to-Kankyo. 49, 30 (2000)
12) Yamashita, M., Sachi, H., Nagano, H., Misawa, T.: Tetsu-to-Haganè. 83, 448 (1997)
13) Sabi Science Kenkyukai: Edited by Jpn. Soc. Corrosion and The Kozai Club (ISIJ), 1999
14) Kimura, M., Suzuki, T., Shigesato, H., Kihira, H., Suzuki, S.: Surface and Interface Analysis. 2002
15) Kimura, M., Suzuki, T., Shigesato, H., Kihira, H., Suzuki, S.: ISIJ International. 42, 1534 (2002)